ELSEVIER

International Journal of Solids and Structures 40 (2003) 7463–7474

INTERNATIONAL JOURNAL OF SOLIDS and STRUCTURES

www.elsevier.com/locate/ijsolstr

Rayleigh–Ritz analysis for localized buckling of a strut on a softening foundation by Hermite functions

G. Chen *, G. Baker [1]

Faculty of Engineering and Surveying, The University of Southern Queensland, West Street, Toowoomba, QLD 4350, Australia

Received 30 January 2003; received in revised form 11 August 2003

Abstract

This paper proposes a Rayleigh–Ritz procedure for localized buckling of a strut on a non-linear elastic foundation. Firstly, the deflected shape of a strut is expanded into a series of Hermite orthogonal functions, which are proved energy-integrable in an infinite region. Secondly, the errors of the numerical integrations of Hermite functions on the infinite region are investigated and the suitable integral limit is proposed. Through the numerical investigation, it is demonstrated that the first thirty Hermite functions are usually enough to approximate the localized buckling pattern. The proposed method overcomes the disadvantages of the traditional methods, in which the trial functions in either Rayleigh–Ritz or Galerkin analysis are based on the perturbation analyses of the corresponding non-linear differential equation.

Keywords: Localized buckling; Non-linear elastic foundation; Hermite functions; Rayleigh–Ritz analysis

1. Introduction

Buried submarine pipelines and continuously welded railway tracks may buckle under axial compression induced by temperature changes. Hobbs (1984) pointed out the similarity between these two kinds of problems. These structures have been modeled as a long beam resting on an elastic foundation and subjected to axial compression (Hetenyi, 1946; Bazant and Cedolin, 1991). A extensive literature has been built-up addressing these structures (Kerr and El-Aini, 1978; Kerr, 1980; Hobbs, 1984; Taylor and Aik Ben, 1984; Raoof and Maschner, 1993; Zhou and Murray, 1996). Often the buckled configuration in such structures is a localized one, with only one or a few buckles (Kerr, 1980; Tvergaard and Needleman, 1981; Hobbs, 1984). The prediction of the behavior of the structures under such circumstances is of significance. Since the local buckling can happen at any location along the length, the successful formulation must admit multiple solutions (Hunt and Wadee, 1991). Among the multiple post-critical equilibrium states, it is the

* Corresponding author. Tel.: +61-7-4631-2299/1713; fax: +61-7-4631-2526.
E-mail addresses: cheng@usq.edu.au (G. Chen), bakerg@usq.edu.au (G. Baker).
[1] Tel.: +61-7-4631-2527; fax: +61-7-4631-2526.

0020-7683/$ - see front matter © 2003 Elsevier Ltd. All rights reserved.
doi:10.1016/j.ijsolstr.2003.08.010

principle of the least energy that governs the real buckled shape, if the structure is under conservative loading (Whiting, 1997).

Both Rayleigh–Ritz method (Wadee et al., 1997) and Galerkin method (Whiting, 1997) have been devoted to this problem. Since randomly selected orthogonal series cannot guarantee the existence of the energy integration, both methods are based on a double-scale perturbation analysis (Thompson and Hunt, 1973; Hunt et al., 1989) to obtain the trial functions or coordinate functions. As its procedure and the resulting trial functions depend on the specific differential equation, the perturbation analysis is merely applicable to a strut with a uniform bending stiffness. Furthermore, the perturbation analysis is only effective when the loading parameter is close to the critical condition. As it is difficult to obtain the higher-order trial functions from the perturbation analysis, the traditional Rayleigh–Ritz, with a few trial functions, fails for the case with re-stabilizing non-linearity (Wadee and Bassom, 2000).

This paper proposes a technique that avoids this dependence upon the perturbation analysis and is capable of generating good approximate solutions throughout the post-buckling regime. Since the buckling shape of a strut is energy-integrable, it can be approximated by a series of orthogonal functions that are also energy-integrable. Hermite functions (Debnath, 1995) are proved orthogonal on an infinite region. This paper will demonstrate that they are complete in a sense and are able to approximate any energy-integrable functions.

This paper first introduces Hermite polynomials and Hermite functions, and the recursion formulae are obtained for Hermite functions and their first and second order derivatives. The expandability of any energy-integrable functions into a series of Hermite functions is discussed. Then, the integration errors of numerical schemes on an infinite region are investigated and a reasonable integration limit is suggested. Finally, numerical examples are used to demonstrate the effectiveness of the technique, and the necessary terms of Hermite functions are investigated.

2. Buckling of a strut on a non-linear elastic foundation

Consider an infinitely long elastic strut of bending stiffness EI, resting on a continuous elastic (Winkler) foundation and loaded by an axial compressive force P, as shown in Fig. 1. The foundation has a softening characteristic which can be introduced either by a piecewise linear function (Tvergaard and Needleman, 1980) or by non-linear components in its stiffness expression (Chater et al., 1983). In this paper, the restoring force F per unit length of the foundation is assumed as

$$F = kw + bw^2 + cw^3 \tag{1}$$

where k represents the linear component of the stiffness, and b and c represent the non-linear components; the softening characteristic is represented by the non-linear components.

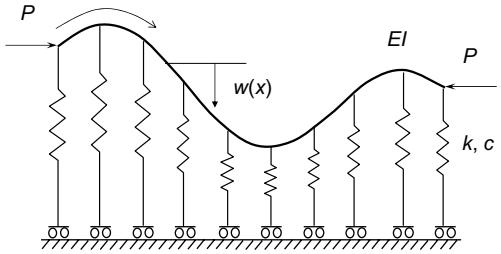

Fig. 1. An elastic strut resting on a non-linear foundation.

The actual response of the strut minimizes the following energy integration:

$$V = \int_{-\infty}^{\infty} \left[\frac{1}{2} EI \left(\frac{\mathrm{d}^2 w}{\mathrm{d}x^2} \right)^2 - \frac{1}{2} P \left(\frac{\mathrm{d}w}{\mathrm{d}x} \right)^2 + \frac{1}{2} k w^2 + \frac{1}{3} b w^3 + \frac{1}{4} c w^4 \right] \mathrm{d}x \tag{2}$$

By introducing the non-dimensional variables $\tilde{x}$, $\widetilde{P}$, $\tilde{w}$, $\tilde{b}$, and $\tilde{c}$ with

$$x = L_c \tilde{x}, \quad P = T_c \widetilde{P}, \quad w = L_c \tilde{w}, \quad b = \tilde{b} k / L_c, \quad c = \tilde{c} k / L_c^2 \tag{3}$$

where

$$L_c = \sqrt[4]{\frac{EI}{k}}, \quad T_c = \sqrt{kEI} \tag{4}$$

the energy integration is simplified as

$$V = \int_{-\infty}^{\infty} k L_c^3 \left\{ \frac{1}{2} \left[\left(\frac{\mathrm{d}^2 \tilde{w}}{\mathrm{d}\tilde{x}^2} \right)^2 - \widetilde{P} \left(\frac{\mathrm{d}\tilde{w}}{d\tilde{x}} \right)^2 + \tilde{w}^2 \right] + \frac{1}{3} \tilde{b} \tilde{w}^3 + \frac{1}{4} \tilde{c} \tilde{w}^4 \right\} \mathrm{d}\tilde{x} \tag{5}$$

Ignoring the trivial constant kL_c^3 and dropping the tildes above x, P, w, b, and c, the problem is changed to minimize

$$V = \int_{-\infty}^{\infty} \left\{ \frac{1}{2} \left[\left(\frac{\mathrm{d}^2 w}{\mathrm{d}x^2} \right)^2 - P \left(\frac{\mathrm{d}w}{\mathrm{d}x} \right)^2 + w^2 \right] + \frac{1}{3} b w^3 + \frac{1}{4} c w^4 \right\} \mathrm{d}x \tag{6}$$

to obtain the buckling shape of the strut. Its corresponding differential equation is

$$w'''' + P w'' + w + b w^3 + c w^3 = 0 \tag{7}$$

where $w'' = \mathrm{d}^2 w / \mathrm{d}x^2$ and $w'''' = \mathrm{d}^4 w / \mathrm{d}x^4$. For the linearized form of Eq. (7), the buckling mode is chosen in the form of $w(x) = A \mathrm{e}^{i\lambda x}$; thus one finds $P = \lambda^2 + 1/\lambda^2$, by minimizing which the critical load $P = 2$ is obtained (Potier-Ferry, 1983).

In practice, the energy stored in the buckling deformation is always finite, which requires that the integration $\int_{-\infty}^{\infty} w^2(x)\,\mathrm{d}x$ exists. In order to obtain a trial function or coordinate functions being able to approximate the actual buckling pattern, the traditional approaches pursue a non-linear double-scale perturbation analysis (Hunt et al., 1989; Wadee et al., 1997) of the differential equation (7). The analysis is merely applicable to a uniform case.

3. Hermite orthogonal functions and their characteristics

To construct a series of coordinate functions being able to approximate the actual buckling pattern, Hermite orthogonal functions, which are standard and irrelevant to a specific structure, are employed.

Hermite orthogonal functions are related to Hermite polynomials. First Hermite polynomials and their orthogonality relation are reviewed, then Hermite orthogonal functions are defined and the recursion formulae are obtained.

3.1. Hermite polynomials

The definition of Hermite polynomials can be found either in Courant and Hilbert (1953) or Poularikas (1996)

$$H_n(t) = (-1)^n e^{t^2} \frac{d^n e^{-t^2}}{dt^n} \quad n = 0, 1, 2, \ldots, \quad -\infty < t < +\infty \tag{8}$$

They satisfy the following relations

$$H_n(-t) = (-1)^n H_n(t) \tag{9}$$

$$H_n'(t) = 2nH_{n-1}(t) \quad n = 1, 2, \ldots \tag{10}$$

and the recursion formula exists,

$$H_n(t) = 2tH_{n-1}(t) - 2(n-1)H_{n-2}(t) \quad n = 2, 3, \ldots \tag{11}$$

Hermite polynomials satisfy the following orthogonality relations (Courant and Hilbert, 1953):

$$\int_{-\infty}^{\infty} e^{-t^2} H_m(t) H_n(t)\, dt = 0 \text{ if } m \neq n \tag{12}$$

and

$$\int_{-\infty}^{\infty} e^{-t^2} H_n(t) H_n(t)\, dt = 2^n n! \sqrt{\pi} \quad n = 0, 1, 2, \ldots \tag{13}$$

3.2. Hermite orthogonal functions

Hermite orthogonal functions (Courant and Hilbert, 1953) are given by

$$F_n(t) = e^{-t^2/2} H_n(t) \quad n = 0, 1, 2, \ldots, \quad -\infty < t < +\infty \tag{14}$$

They are also called Weber–Hermite orthogonal functions (Debnath, 1995). From (12) and (13) it can be seen that they satisfy the following orthogonality relations:

$$\int_{-\infty}^{\infty} F_m(t) F_n(t)\, dt = 0 \text{ if } m \neq n \tag{15}$$

and

$$\int_{-\infty}^{\infty} F_n(t) F_n(t)\, dt = 2^n n! \sqrt{\pi} \quad n = 0, 1, 2, \ldots \tag{16}$$

Hence, the normalized Hermite functions are defined as

$$\widehat{F}_n(t) = \frac{1}{\sqrt{2^n n! \sqrt{\pi}}} F_n(t) = \frac{1}{\sqrt{2^n n! \sqrt{\pi}}} e^{-t^2/2} H_n(t) \tag{17}$$

The first six normalized Hermite functions (for $n = 0$–5) are shown in Fig. 2. Obviously, Hermite functions attenuate very fast, which means they are ideal coordinate functions to represent the localized buckling pattern.

Eqs. (9) and (11) show that Hermite functions satisfy

$$F_n(-t) = (-1)^n F_n(t) \tag{18}$$

and also the following recursion formula exists

$$F_n(t) = 2tF_{n-1}(t) - 2(n-1)F_{n-2}(t) \quad n \geqslant 2 \tag{19}$$

By differentiating (14) and making use of (10) and (14), the recursion formula is obtained for the first order derivatives of Hermite functions:

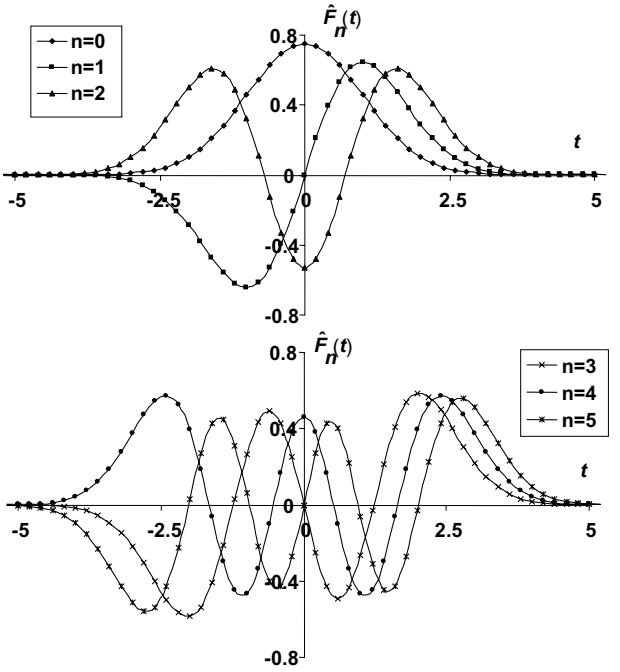

Fig. 2. The normalized Hermite functions.

$$F_n'(t) = 2nF_{n-1}(t) - tF_n(t) \quad n \geqslant 1 \tag{20}$$

By differentiating (20) and using (20) repeatedly, the recursion formula is derived for the second order derivatives:

$$F_n''(t) = 4n(n-1)F_{n-2}(t) - 4ntF_{n-1}(t) + (t^2-1)F_n(t) \quad n \geqslant 2 \tag{21}$$

Hence, from the first two Hermite orthogonal functions, the higher-order functions and their first and second order derivatives can be computed from the recursion formulae. For the convenience of computation, Table 1 lists the first two Hermite orthogonal functions, their first and second order derivatives, and the recursion formulae for higher-order orthogonal functions and their derivatives.

By assuming that $F_{(-1)}(t)$ and $F_{(-2)}(t)$ exist, it is easy to check that the recursion formulae for the derivatives $F_n'(t)$ and $F_n''(t)$ are valid even for $n = 0$ and $n = 1$. Hence, by assuming $F_{(-2)}(t) = F_{(-1)}(t) = 0$, all the derivatives $F_n'(t)$ and $F_n''(t)$ can be obtained from $F_n(t)$ by making use of the recursion formulae.

In numerical calculation, the value of $F_n(t)$ may become very large when n is big. It is more convenient to use the normalized Hermite functions. The recursion formulae for the normalized Hermite functions are listed in Table 2.

Table 1
Recursion formulae of Hermite orthogonal functions

n	0	1	$n \geqslant 2$
$F_n(t)$	$e^{-t^2/2}$	$2te^{-t^2/2}$	$2tF_{n-1}(t) - 2(n-1)F_{n-2}(t)$
$F_n'(t)$	$-te^{-t^2/2}$	$2(1-t^2)e^{-t^2/2}$	$2nF_{n-1}(t) - tF_n(t)$
$F_n''(t)$	$(t^2-1)e^{-t^2/2}$	$(2t^3-6t)e^{-t^2/2}$	$4n(n-1)F_{n-2}(t) - 4ntF_{n-1}(t) + (t^2-1)F_n(t)$

Table 2
Recursion formulae of normalized Hermite orthogonal functions

n	0	1	$n \geqslant 2$
$\widehat{F}_n(t)$	$\frac{1}{\sqrt[4]{\pi}}\mathrm{e}^{-t^2/2}$	$\frac{1}{\sqrt{2\sqrt{\pi}}}2t\mathrm{e}^{-t^2/2}$	$\sqrt{\frac{2}{n}}t\widehat{F}_{n-1}(t) - \sqrt{\frac{n-1}{n}}\widehat{F}_{n-2}(t)$
$\widehat{F}'_n(t)$	$-\frac{1}{\sqrt[4]{\pi}}t\mathrm{e}^{-t^2/2}$	$\frac{1}{\sqrt{2\sqrt{\pi}}}2(1-t^2)\mathrm{e}^{-t^2/2}$	$\sqrt{2n}\widehat{F}_{n-1}(t) - t\widehat{F}_n(t)$
$\widehat{F}''_n(t)$	$\frac{1}{\sqrt[4]{\pi}}(t^2-1)\mathrm{e}^{-t^2/2}$	$\frac{1}{\sqrt{2\sqrt{\pi}}}(2t^3-6t)\mathrm{e}^{-t^2/2}$	$2\sqrt{n(n-1)}\widehat{F}_{n-2}(t) - 2\sqrt{2n}t\widehat{F}_{n-1}(t) + (t^2-1)\widehat{F}_n(t)$

3.3. Expansion in Hermite orthogonal functions

Any function, $f(t)$, which is energy integrable, can be expanded into a converged series of Hermite orthogonal functions. It can be proved via the completeness of a Hermite polynomial series.

If a continuous function, $h(t)$, satisfies $\int_{-\infty}^{\infty}\mathrm{e}^{-t^2}h^2(t)\,\mathrm{d}t < \infty$, its Hermite polynomial series

$$h(t) = \sum_{n=0}^{\infty} C_n H_n(t) \quad -\infty < t < \infty \tag{22}$$

with the coefficients

$$C_n = \frac{1}{2^n n!\sqrt{\pi}}\int_{-\infty}^{\infty}\mathrm{e}^{-t^2}h(t)H_n(t)\,\mathrm{d}t \tag{23}$$

converges to $h(t)$ (Poularikas, 1996).

Let

$$f(t) = \mathrm{e}^{-t^2/2}h(t) \tag{24}$$

Then $f(t)$ satisfies $\int_{-\infty}^{\infty}f^2(t)\,\mathrm{d}t < \infty$. By multiplying $\mathrm{e}^{-t^2/2}$ on the both sides, Eq. (22) can be changed into

$$f(t) = \sum_{n=0}^{\infty} C_n F_n(t) \quad -\infty < t < \infty \tag{25}$$

Obviously (23) can be re-written as

$$C_n = \frac{1}{2^n n!\sqrt{\pi}}\int_{-\infty}^{\infty}f(t)F_n(t)\,\mathrm{d}t \tag{26}$$

From the convergence of Eq. (22), it can be seen that Eq. (25) converges to $f(t)$. Since $h(t)$ is any continuous function that satisfies $\int_{-\infty}^{\infty}\mathrm{e}^{-t^2}h^2(t)\,\mathrm{d}t < \infty$, thus any continuous function, $f(t)$, which satisfies $\int_{-\infty}^{\infty}f^2(t)\,\mathrm{d}t < \infty$, can be expanded into a converged series of Hermite orthogonal functions. For our case, $\int_{-\infty}^{\infty}f^2(t)\,\mathrm{d}t$ represents the energy integration that must be finite.

If normalized Hermite orthogonal functions are used, the expansion becomes:

$$f(t) = \sum_{n=0}^{\infty}\widehat{C}_n\widehat{F}_n(t), \quad \widehat{C}_n = \int_{-\infty}^{\infty}f(t)\widehat{F}_n(t)\,\mathrm{d}t \tag{27}$$

4. Numerical analyses

According to the theoretical analysis above, the deflection, $w(x)$, which satisfies $\int_{-\infty}^{\infty}w^2(x)\,\mathrm{d}x < \infty$, can be approximated by a series of Hermite orthogonal functions

$$\bar{w}(x) = \sum_{n=0}^{N} \widehat{C}_n \widehat{F}_n(x) \quad -\infty < x < \infty \tag{28}$$

and its derivatives are

$$\bar{w}'(x) = \sum_{n=0}^{N} \widehat{C}_n \widehat{F}'_n(x), \quad \bar{w}''(x) = \sum_{n=0}^{N} \widehat{C}_n \widehat{F}''_n(x) \tag{29}$$

By substituting (28) and (29) into (6), the potential energy functional (6) is reduced to a polynomial of $\widehat{C}_0, \widehat{C}_1, \widehat{C}_2, \ldots, \widehat{C}_N$,

$$V = V(\widehat{C}_0, \widehat{C}_1, \widehat{C}_2, \ldots, \widehat{C}_N) \tag{30}$$

The relevant amplitudes are to be found by minimizing the potential energy function (30) (i.e., solving the equilibrium equations of the Rayleigh–Ritz model). Accuracy depends on the number of coordinate functions and the ability of the chosen functions to represent the actual buckling pattern.

4.1. Limits of integration

Eq. (30) involves the energy integration on the infinite region $-\infty < x < \infty$. It mainly involves the integration of $\int_{-\infty}^{\infty} \widehat{F}_m(x)\widehat{F}_n(x)\,\mathrm{d}x$, $\int_{-\infty}^{\infty} \widehat{F}_m(x)\widehat{F}_n^3(x)\,\mathrm{d}x$, and $\int_{-\infty}^{\infty} \widehat{F}_m^2(x)\widehat{F}_n^2(x)\,\mathrm{d}x$. For numerical analyses, an appropriate integral limit, α, has to be determined and the integral $\int_{-\infty}^{\infty} \widehat{F}_m(x)\widehat{F}_n(x)\,\mathrm{d}x$ can be approximated by $\int_{-\alpha}^{\alpha} \widehat{F}_m(x)\widehat{F}_n(x)\,\mathrm{d}x$. Their integration accuracies can be represented by those of $\int_{-\alpha}^{\alpha} \widehat{F}_n^2(x)\,\mathrm{d}x$ and $\int_{-\alpha}^{\alpha} \widehat{F}_n^4(x)\,\mathrm{d}x$. In order to decide the integration limit, α, two functions are defined to measure the integration errors:

$$\mathrm{Error2}(n,\alpha) = 1 - \frac{\int_{-\alpha}^{\alpha} \widehat{F}_n^2(x)\,\mathrm{d}x}{\int_{-\infty}^{\infty} \widehat{F}_n^2(x)\,\mathrm{d}x}, \quad \mathrm{Error4}(n,\alpha) = 1 - \frac{\int_{-\alpha}^{\alpha} \widehat{F}_n^4(x)\,\mathrm{d}x}{\int_{-\infty}^{\infty} \widehat{F}_n^4(x)\,\mathrm{d}x} \tag{31}$$

(It should be noted that $\int_{-\infty}^{\infty} \widehat{F}_n^2(x)\,\mathrm{d}x = 1$ and $\int_{-\infty}^{\infty} \widehat{F}_n^4(x)\,\mathrm{d}x$ is calculated with the integration limit being very large.) The variation of $\mathrm{Error2}(n,\alpha) \sim n$ for $\alpha = 5$–9 is shown in Fig. 3. It is obvious that for the same integral limit α, $\int_{-\alpha}^{\alpha} \widehat{F}_n^2(x)\,\mathrm{d}x$ has different accuracy for a different n. In order to achieve a similar accuracy, α should increase with n. If $\alpha = \mathrm{int}(4\sqrt[3]{n})$ is used, the integral errors for $\int_{-\alpha}^{\alpha} \widehat{F}_n^2(x)\,\mathrm{d}x$ and $\int_{-\alpha}^{\alpha} \widehat{F}_n^4(x)\,\mathrm{d}x$ are listed in Table 3 for $n = 5$–180. (Here the function int( ) rounds the number down to the nearest integer.) From Table 3, it can be seen, for $\alpha = \mathrm{int}(4\sqrt[3]{n})$, $\int_{-\alpha}^{\alpha} \widehat{F}_n^2(x)\,\mathrm{d}x$ and $\int_{-\alpha}^{\alpha} \widehat{F}_n^4(x)\,\mathrm{d}x$ keep a similar accuracy for all n.

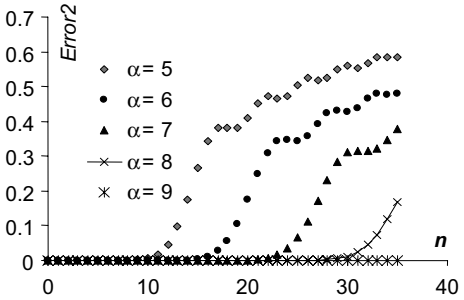

Fig. 3. The integration errors for different α.

Table 3
The integration errors

n	5	10	15	20	30	50	99	180
$\alpha = \mathrm{int}(4\sqrt[3]{n})$	6	8	9	10	12	14	18	22
Error2(n,α)	2.9E−10	1.1E−16	1.3E−15	8.9E−16	6.7E−16	4.4E−16	1.9E−15	6.7E−15
Error4(n,α)	7.8E−16	1.2E−15	1.1E−15	2.2E−16	6.7E−16	8.9E−16	1.1E−16	1.2E−15

Hence, in the numerical analyses, $\alpha = \mathrm{Max}(\mathrm{int}(4\sqrt[3]{N}), 6)$, i.e., the lager of $\mathrm{int}(4\sqrt[3]{N})$ and 6, is used as the integral limit. Here N is the order of the highest-order Hermite orthogonal function.

4.2. Numerical scheme

In this paper, Simpson's integration scheme is used and the integration is carried on $[-\alpha, \alpha]$. If the number of integral points within one unit length is represented by M ($=20$–50 in this paper), the integral step length is $1/M$, and the integration points are at $x_i = i/M$ where i varies from $-M\alpha$ to $M\alpha$. The energy integration (6) is approximated by

$$V = \sum_{i=-M\alpha}^{M\alpha} \left\{ \begin{array}{l} \frac{1}{2}\left[\sum_{n=0}^{N} \widehat{C}_n \widehat{F}_n''(x_i)\right]^2 - \frac{1}{2}P\left[\sum_{n=0}^{N} \widehat{C}_n \widehat{F}_n'(x_i)\right]^2 + \frac{1}{2}\left[\sum_{n=0}^{N} \widehat{C}_n \widehat{F}_n(x_i)\right]^2 \\ +\frac{1}{3}b\left[\sum_{n=0}^{N} \widehat{C}_n \widehat{F}_n(x_i)\right]^3 + \frac{1}{4}c\left[\sum_{n=0}^{N} \widehat{C}_n \widehat{F}_n(x_i)\right]^4 \end{array} \right\} \cdot \frac{1}{M} \tag{32}$$

Since the approximate potential surface (32) is an analytical function of the amplitudes $\widehat{C}_0, \widehat{C}_1, \widehat{C}_2, \ldots, \widehat{C}_N$. Its minima can be found by using a multi-dimensional Newton–Raphson method (Press et al., 1992). By making use of the vector expression, the Newton–Raphson iteration is stated as

$$\widehat{\mathbf{C}}_{\mathrm{new}} = \widehat{\mathbf{C}}_{\mathrm{old}} - \mathbf{H}^{-1}\mathbf{F} \tag{33}$$

where

$$\mathbf{H} = \frac{\partial^2 V}{\partial \widehat{C}_i \partial \widehat{C}_j}(\widehat{\mathbf{C}}_{\mathrm{old}}), \quad \mathbf{F} = \frac{\partial V}{\partial \widehat{C}_i}(\widehat{\mathbf{C}}_{\mathrm{old}}) \tag{34}$$

are the values of Hessian matrix and gradient of potential energy at the previous trial solution.

4.3. Numerical examples

(1) Comparison with the perturbation solution (with $b = 0$ and $c = -1$). If the loading parameter P is close to the critical value $P_c = 2$, the perturbation solution is valid. Under this circumstance, the perturbation solution varies in a considerable length; on the other hand, Hermite functions attenuate fast. In order to approximate the buckling mode accurately, many terms of Hermite functions are needed. Because of the symmetry of the buckling mode, the odd terms of Hermite orthogonal functions are superfluous. Only the first 91 even terms are used, i.e., $N = 180$. The comparison of the Rayleigh–Ritz approach and the perturbation solution is shown in Fig. 4 for three different loads in the range of $0 \leqslant P < P_c$. For the case of $P = 1.95$, the perturbation solution is quite accurate; the Rayleigh–Ritz solution is very close to the perturbation solution in the range $[-19, 19]$, beyond which the Rayleigh–Ritz solution attenuates quickly. For the case of $P = 1.90$, the solutions by two approaches are quite close, since the perturbation solution also attenuates faster. For the case of $P = 1.80$, the solutions by two approaches have an obvious difference

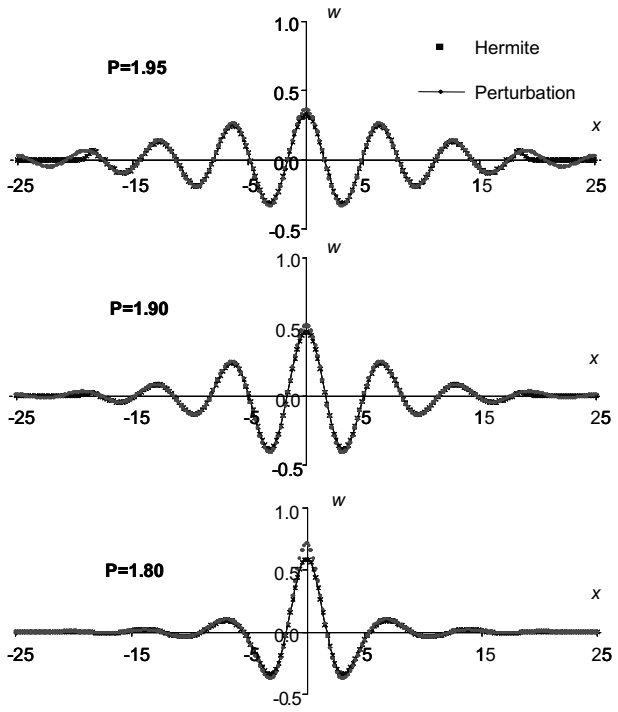

Fig. 4. Comparison of the Rayleigh–Ritz analysis of Hermite function with perturbation solution (Wadee et al., 1997), with $b = 0$ and $c = -1$.

around the origin point, since the perturbation solution is no longer accurate for this case (Whiting, 1997) that is not close to the critical condition ($P = 2.00$).

(2) Comparison with Galerkin approach (with $b = 0$ and $c = -1$). For the case that the loading parameter P is not close to the critical value, the perturbation solution is invalid. Whiting (1997) has demonstrated by Galerkin method that the solution is quite localized. Hence, a few of Hermite functions are able to approximate the buckling mode accurately. For this case, the first 26 even terms are employed, i.e., $N = 50$. The comparison of the Rayleigh–Ritz approach and the results of Whiting (1997) are shown in Fig. 5 for $P = 1.00$ and 0.00. The results of the two approaches are very close.

(3) The convergence of the solutions (with $b = 0$ and $c = -1$). For the case of $P = 1.00$ and 0.00, let the coordinate function numbers $N = 50$, 30, 10, the corresponding buckling shapes are shown in Fig. 6. The buckling shapes for $N = 50$ and 30 almost completely overlap each other, which means the solutions have a good convergence. Hence, generally, the first sixteen even terms ($N = 30$) is able to model the buckling pattern accurately. Even with only six even terms ($N = 10$) the solution are quite acceptable.

(4) Comparison with AUTO solutions (with $b = -1$). In the case with re-stabilizing non-linearity (Wadee and Bassom, 2000), the buckling mode undergoes a series of oscillations. As it is difficult to obtain the higher-order trial functions from perturbation analysis, thus, with only a few perturbation trial functions, the Rayleigh–Ritz analysis fails for this case. In the proposed approach, as trial functions, Hermite functions, are known, it is expected that, with enough trial functions, the Rayleigh–Ritz approach is applicable to this case. The results are shown in Fig. 7 with the comparisons with other numerical solutions (AUTO). For two cases with ($P = 1.20$, $c = 0.24$) and ($P = 1.74$, $c = 0.40$), the results of the Rayleigh–Ritz analysis with the first 51 even Hermite functions are very close to AUTO solutions (Wadee and Bassom,

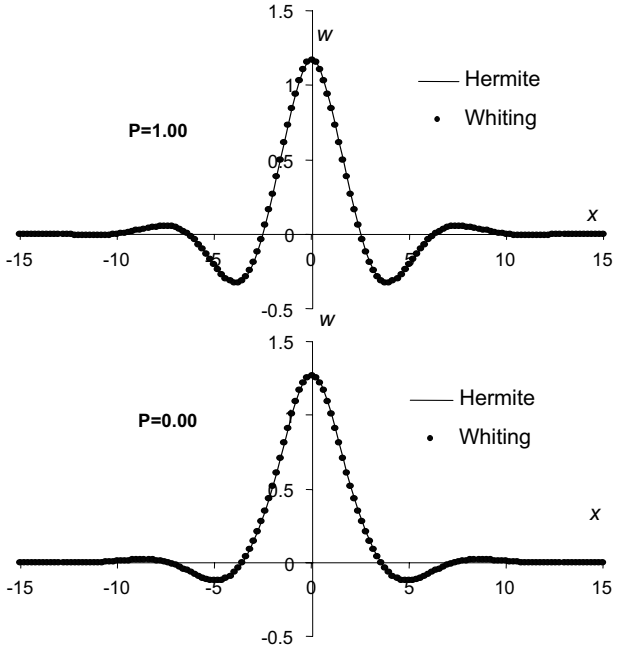

Fig. 5. Comparison of the Rayleigh–Ritz analysis of Hermite function with Galerkin analysis (Whiting, 1997), with $b = 0$ and $c = -1$.

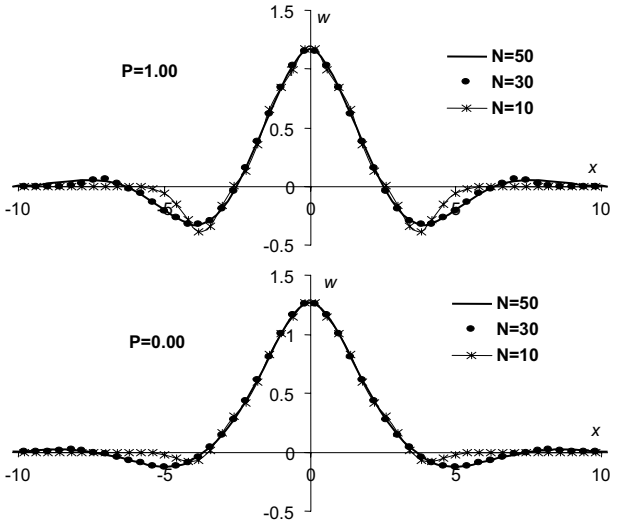

Fig. 6. Convergence of the solutions by Hermite functions, with $b = 0$ and $c = -1$.

2000) except at the points outside the range of $[-15, 15]$; with the first 91 even Hermite functions, the differences between the Rayleigh–Ritz solutions and AUTO solutions are indistinguishable.

(5) The efficiency of the techniques. The proposed method is efficient. For the case of $N = 180$, the computational time on a personal computer is only 4.35 min. For $N \leqslant 50$, the computational time is less than 1.0 min.

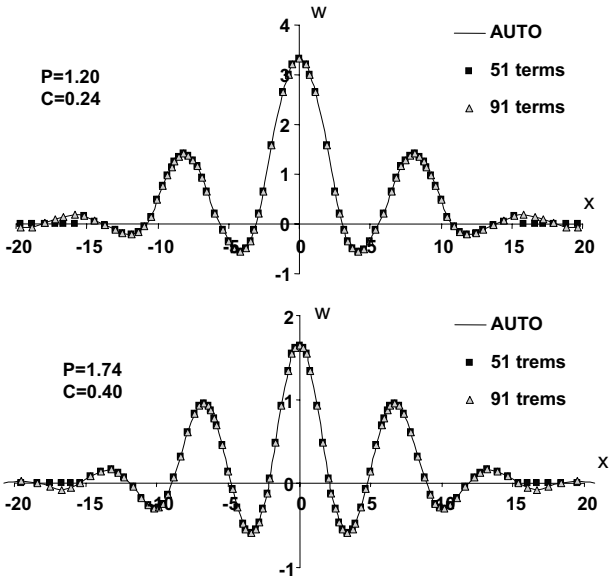

Fig. 7. Comparison of the Rayleigh–Ritz analysis of Hermite functions with AUTO solutions for re-stabilization (with $b = -1$).

5. Conclusions

This paper has presented a Rayleigh–Ritz procedure for localized buckling of a strut on a non-linear elastic foundation. The deflected shape of a strut is expanded as a series of Hermite orthogonal functions. The recursion formulae for Hermite orthogonal functions and their derivatives have been derived. The expandability of an energy-integrable function into a series of Hermite orthogonal functions has been proved. The errors of the numerical integration of Hermite functions on an infinite region have been investigated and a reasonable integral limit, $\alpha = \mathrm{Max}(\mathrm{int}(4\sqrt[3]{N}), 6)$, has been suggested. Through the numerical investigation, the following conclusions could be reached:

(1) The localized buckling pattern can be approximated by a series of Hermite orthogonal functions. The proposed method overcomes the disadvantages of the traditional methods, in which the trial functions for either Rayleigh–Ritz or Galerkin approach are based on the perturbation analyses of the corresponding non-linear differential equation. With enough trial functions, the proposed Rayleigh–Ritz approach is applicable to the case with re-stabilizing non-linearity where the traditional Rayleigh–Ritz analysis fails.

(2) The proposed method is efficient and has a good convergence. The first sixteen even terms are able to model the buckling pattern accurately. Even for the case in which the buckling mode varies in a considerable length, only the first ninety-one even terms are enough to approximate the buckling mode. In the numerical sense, this computational load is very little. As Hermite functions are standard and less than one hundred terms are employed, with a little effort, the proposed method can be implemented in a personal computer.

References

Bazant, Z.P., Cedolin, L., 1991. Stability of Structures: Elastic, Inelastic, Fracture, and Damage Theories. Oxford University Press, New York.

Chater, E., Hutchinson, J.W., Neale, K.W., 1983. Buckle propagation on a beam on a nonlinear elastic foundation. In: Thompson, J.M.T., Hunt, G.W. (Eds.), Collapse: The Buckling of Structures in Theory and Practice. Cambridge University Press, Cambridge, pp. 31–41.

Courant, R., Hilbert, D., 1953. Methods of Mathematical Physics. Interscience Publishers, New York.

Debnath, L., 1995. Integral Transforms and their Applications. CRC Press, Boca Raton.

Hetenyi, M.I., 1946. Beams on Elastic Foundation: Theory with Applications in the Fields of Civil and Mechanical Engineering. University of Michigan Press, Ann Arbor.

Hobbs, R.E., 1984. In-service buckling of heated pipelines. Journal of Transportation Engineering 110 (2), 175–189.

Hunt, G.W., Wadee, M.K., 1991. Comparative Lagrangian formulations for localized buckling. Proceedings of the Royal Society of London, Series A: Mathematical, Physical and Engineering Sciences 434, 485–502.

Hunt, G.W., Bolt, H.M., Thompson, J.M.T., 1989. Structural localization phenomena and the dynamical phase-space analogy. Proceedings of the Royal Society of London, Series A: Mathematical and Physical Sciences 425, 245–267.

Kerr, A.D., 1980. Improved analysis for thermal track buckling. International Journal of Non-linear Mechanics 15 (2), 99–114.

Kerr, A.D., El-Aini, Y.M., 1978. Determination of admissible temperature increases to prevent vertical track buckling. Journal of Applied Mechanics, Transactions ASME 45 (3), 565–573.

Potier-Ferry, E., 1983. Amplitude modulation, phase modulation and localization of buckling patterns. In: Thompson, J.M.T., Hunt, G.W. (Eds.), Collapse: The Buckling of Structures in Theory and Practice. Cambridge University Press, Cambridge, pp. 149–159.

Poularikas, A.D., 1996. The Transforms and Applications Handbook. CRC Press, Boca Raton Fla.

Press, W.H., Flannery, B.P., Teukolsky, S.A., Vetterling, W.T., 1992. Numerical Recipes in FORTRAN: The Art of Scientific Computing. Cambridge University Press, Cambridge, UK.

Raoof, M., Maschner, E., 1993. Thermal buckling of subsea pipelines. In: Proceedings of the International Conference on Offshore Mechanics and Arctic Engineering—OMAE, Glasgow.

Taylor, N., Aik Ben, G., 1984. Regarding the buckling of pipelines subject to axial loading. Journal of Constructional Steel Research 4 (1), 45–50.

Thompson, J.M.T., Hunt, G.W., 1973. A General Theory of Elastic Stability. Wiley, London.

Tvergaard, V., Needleman, A., 1980. On the localization of buckling patterns. Journal of Applied Mechanics, Transactions ASME 47 (3), 613–619.

Tvergaard, V., Needleman, A., 1981. On localized thermal track buckling. International Journal of Mechanical Sciences 23 (10), 577–587.

Wadee, M.K., Bassom, A.P., 2000. Restabilization in structures susceptible to localized buckling: an approximate method for the extended post-buckling regime. Journal of Engineering Mathematics 38 (1), 77–90.

Wadee, M.K., Hunt, G.W., Whiting, A.I.M., 1997. Asymptotic and Rayleigh–Ritz routes to localized buckling solutions in an elastic instability problem. Proceedings of the Royal Society of London, Series A: Mathematical, Physical and Engineering Sciences 453 (1965), 2085–2107.

Whiting, A.I.M., 1997. Galerkin procedure for localized buckling of a strut on a nonlinear elastic foundation. International Journal of Solids and Structures 34 (6), 727–739.

Zhou, Z., Murray, D.W., 1996. Pipeline beam model using stiffness property deformation relations. Journal of Transportation Engineering 122 (2), 164–172.